ORIGINAL RESEARCH

Microdamage Accumulation Changes According to Animal Mass: An Intraspecies Investigation

Stefano Z. M. Brianza · Patrizia D'Amelio · Nicola Pugno ·
Eric Zini · Andrea Zatelli · Fernanda Pluviano ·
Karine Cabiale · Marco Galloni · Giovanni Carlo Isaia

Abstract The fatigue life of a structure is also influenced by its size. Statistically, a bone from a large animal is expected to bear a higher risk of stress fracture if compared to the same bone from a small animal of the same species. This is not documented in the dog, where individuals can have a 40 times difference in body mass. We investigated the effect of body size on cortical bone microdamage accumulation, cortical microstructural organization (porosity, osteon area, and osteocyte lacunar density), and turnover in dogs with a wide body mass range. The aim was to understand and mathematically model how the bone tissue copes with the microdamage accumulation linked to body mass increase. Calcified transverse cortical sections of 18 canine radii of remarkably different size were examined by means of a standard bulk-staining technique and histomorphometric standard algorithms. Relationships between the investigated histomorphometric variables age, sex and mass were analyzed by general linear multivariate models and exponential equations. Type and location of microdamage and bone turnover were not influenced by body mass. Gender did not influence any parameter. Age influenced bone turnover and activation frequency. Microcrack density was influenced by bone mass. Bones had a similar microstructural organization within the same species regardless of the subject's dimension. Microdamage accumulation is inversely related to bone mass, whereas bone turnover is mass-invariant. We theorize a mass-related change in the bone fracture toughness targeted to reach an optimal unique dimensionless curve for fatigue life.

Keywords Microdamage · Scaling · Size effect · Bone material property · Fatigue

S. Z. M. Brianza (✉) · P. D'Amelio · G. C. Isaia
Department of Surgical and Medical Disciplines,
Section of Gerontology, University of Torino,
Corso Bramante 88/90, 10126 Torino, Turin, Italy
e-mail: stefanobrianza@yahoo.it

N. Pugno
Department of Structural Engineering and Geotechnics,
Politecnico di Torino, Turin, Italy

K. Cabiale · M. Galloni
Department of Morphophysiology, Faculty of Veterinary
Medicine, University of Torino, Turin, Italy

E. Zini
Clinic for Small Animal Internal Medicine, Vetsuisse Faculty,
University of Zürich, Zurich, Switzerland

A. Zatelli
"Pirani" Veterinary Clinic, Reggio Emilia, Italy

F. Pluviano
Department of Imaging, Faculty of Medicine,
University of Torino, Turin, Italy

Cyclic stresses produce an incremental failure process in the form of accumulation of matrix microdamage prior to bone collapse [1–4]. The effect of these repeated stresses in animal bones has been widely investigated, and fatigue fractures are a common consequence in animal athletes, especially thoroughbred horses [5] and greyhound dogs [3]. In general, the fatigue life of a generic structure is influenced by its loading history, by the quality of its material, and by its size. Generally speaking, larger components are

more prone to fatigue failure since a greater stressed volume implies a higher probability of finding a weak region where a crack forms, grows, and leads to failure of the entire structure; this size effect has been described in compact bone as well [6]. Based on these observations, a bone from a large animal is expected to have (1) an increase in microdamage accumulation and, thus, a higher risk of stress fracture than the same bone from a small animal of the same species or (2) the same risk of stress fracture but with different tissue organization or properties. In the canine species we have the chance to test this hypothesis in individuals with a common genetic ancestry [7] and a unique 40-fold difference in body mass. Microdamage accumulation from physiological loading has been described in this species [2, 3, 8, 9], but a mass-related incidence of stress fractures was not found. In our previous studies on the features of bones and their structural failure properties within a species [10, 11], we showed that allometric scaling of the bone length and the cross-sectional layout, without an increase in the amount of material proportionally employed, preserves linear with the animal mass the amount of energy necessary to fracture a bone and restrain the rise of stresses and strains in the cross section. This mass-driven dimensional optimization might imply a higher microdamage accumulation, but the absence of mass-related fatigue fracture incidence in dogs suggests that the microdamage accumulation is somehow mass-optimized as well.

The purpose of the present study was to examine the microstructural organization of the cortical bone tissue and naturally occurring fatigue microdamage in ground sections of bones from animals of the same species but of remarkably different size. Our goal was to determine whether the cortical bone damage status or the cortical microstructure—namely, porosity, osteon area, and osteocyte lacunar density—change with increasing animal mass. Furthermore, we assessed whether any of the investigated variables could explain how the bone tissue copes with an increased risk of microdamage accumulation related to larger bone sizes. Besides the experimental work, we discuss in the appendix (supplementary material) a mathematical model that, starting from the retrieved data, provides a theoretical explanation of how the bone tissue could dampen an increase in microdamage accumulation with an increase of the bone structure size.

Methods

Experimental Subjects

We collected 18 radii from entire fully grown dogs (age 9.8 ± 4.1 years [range 3–17]; nine females, nine males; body mass 17.7 ± 13 kg [range 2.5–45]) that died naturally or were euthanized due to causes unaffecting bone integrity. To take into account the influence of size on life expectancy [12, 13], we also expressed ages (t, years), determined from medical records, as the ratio between the age of each individual and the expected life span typical for its mass (normalized age t*, %). According to Greer et al. [14], we calculated life expectancy from the following equation: $y = 13.620 + (0.0072 * x_{G}) - (0.0538 * x_{W})$, where y is the expected life span, x_{G} is the dog height, and x_{W} is the dog mass. There was no history of fracture, angular deformities, or forelimb lameness in the sample population. Sixteen percent of the dogs were mongrels; the others were pure-breed dogs ranging from Yorkshire terriers to rottweilers.

Body and Bone Mass

We determined body mass on a standard balance with a precision of 0.5 kg. The foreleg was harvested, the soft tissues were removed, and the radial mass was determined with a balance, with a precision of 0.01 g. Bones were then wrapped in saline-soaked towels and frozen at −20°C until processed.

Histomorphometry

A 1-cm bone segment centered at 30% of the distoproximal radial length was excised, defatted in chloroform for 2 days, and then fixed in 70% ethanol. Specimens were bulk-stained in 1% basic fuchsin in a graded series of alcohols (80%, 90%, 100%) under a vacuum of 20 mmHg for 18 days. Stained specimens were then rinsed in 100% ethanol, infiltrated with washed methyl methacrylate monomer for 10 days under a vacuum of 20 mmHg, and embedded in methy-butylmethacrylate (Sigma-Aldrich, St. Louis, MO). Three transverse sections were prepared for each bone segment with a diamond saw (IsoMet; Buehler, Lake Bluff, IL) and reduced to a thickness of 150 μm with a grinder (Mecapol 2B; Presi, Grenoble, France) and sandpaper.

Fields of interest were filmed with a color video camera (DFC320; Leica, Deerfield, IL). A single observer collected the following data with the UTHSCSA image analysis software (developed by Willcox et al. at the University of Texas, Health Science Center, San Antonio, Texas; maxrad6.uthscsa.edu). Histomorphometric analyses were performed in agreement with the standard nomenclature [15].

Morphometric Analysis

Morphometric analysis was performed in bright light at 200× magnification. The data for three calcified sections

were averaged for each dog according to the literature [1, 2]. *Microcracks* were defined as linear structures with sharp borders, some depth of field, and basic fuchsin staining around. We did not measure diffuse staining of the matrix, and unstained cracks were regarded as artifacts associated with tissue processing, as previously suggested [9, 16]. The following histomorphometric variables were measured, according to Schaffler et al. [1]: bone area (B.Ar, mm^2), microcrack density (Cr.Dn, n/mm^2), and microcrack mean length (Cr.Le, μm). Microcrack morphology was classified according to Norman and Wang [17] as follows: type 1, microcrack in the interstitial bone matrix; type 2, microcrack extending between the matrix and the cement line; type 3, microcrack along the cement line; type 4, interlamellar microcrack; type 5, microcrack within the osteon approaching, but not reaching, the cement line; type 6, microcrack within the osteon terminating at the cement line; and type 7, microcrack crossing the cement line.

Osteocyte Lacunar Density

We counted osteocyte lacunae using blue-violet epifluorescent light (425–440 excitation and 475-nm barrier filter) within five fields per quadrant at 400× and calculated the osteocyte lacunar density (Oc.Dn, number/mm^2). Lacunae were identified from the presence of fluorescence at their edges and the canalicular processes [18].

Porosity

We calculated porosity, expressed as a percentage, as the ratio between the void and the total area (Vd.Ar/T.Ar, %) in four fields per quadrant in bright light at 100× in each of four quadrants (Vd.Ar/T.Ar$_{\text{cranial, caudal, medial, lateral}}$, %). Void areas included resorption and vascular spaces.

Bone Turnover

We estimated the activation frequency (Ac.f, n/mm^2/year) and bone-formation rate (BFR/BV, mm^3/mm^3/year) using the following standard algorithm [19]:

$$\text{Ac.f} = \frac{[\beta(\text{On.N.Int} + \text{On.N.Fg})]}{t}$$

where t is age (years) and

$$\beta = \left\{ 1 - \left[\left(\frac{\text{On.N.Int} + \text{On.N.Fg}}{(\text{On.Ar})^{-1}} \right) \right]^{3,5} \right\}^{-1}$$

We calculated bone formation rate as BFR/BV = Ac.f * On.Ar. We performed measurements in four fields of view in bright light at 100× in each of four quadrants

(cranial, caudal, medial, and lateral). Mean tissue age [20] was taken as the chronological age. As the role of osteon size and number in the control of crack propagation is unclear, we measured the mean osteon area (On.Ar, mm^2 [25 complete osteons]) and the number of intact (On.N.Int, n/mm^2 [>90% of perimeter intact]) and fragmentary (On.N.Fg, n/mm^2 [>10% of perimeter remodeled]) osteons.

Statistics

Statistics were analyzed using SPSS 17.0 for Windows (SPSS, Inc., Chicago, IL). Relationships between the investigated histomorphometric variables, t^*, and bone mass were analyzed by a general linear multivariate (GLM) multivariate model using sex as a fixed factor. Correlations between cortical microstructure and microcrack density and length were estimated by Pearson's coefficient. In order to evaluate the relationship between histomorphometric parameters (microdamage status, cortical microstructure, and bone turnover), age, bone mass, and sex, we ran a second GLM using age and bone mass as covariates and sex as a fixed factor. Additionally, we described with exponential equations the relationship between t^*, bone mass, and the variables found significant using the GLM. The significance cut-off was $P < 0.05$.

Theoretical Model

Starting from the experimental data retrieved, we propose in the appendix (supplementary material) a mathematical model that provides a theoretical explanation of how the bone tissue could dampen an increase in microdamage accumulation with an increase of the size of the bone structure.

Results

Table 1 shows mean and standard deviation parameters for bone mass, body mass, age, and normalized age as distributed according to sex.

Microcrack density and length, osteocyte lacunar density, mean osteon area, bone porosity, and estimation of the

Table 1 Mean and standard deviation parameters for the investigated population according to gender

	Males ($n = 9$)	Females ($n = 9$)
Bone mass (g)	32.05 ± 22.36	26.23 ± 17.89
Body mass (kg)	18.39 ± 15.15	16.94 ± 11.30
Age (years)	10.11 ± 4.14	9.56 ± 4.39
Normalized age (%)	76 ± 27	72 ± 31

Table 2 Mean and standard deviation for the investigated histo-morphometric parameters

Measured parameter	Mean ± SD
Microcrack density (n/mm^2)	0.06 ± 0.04
Microcracks mean length (mm)	0.06 ± 0.02
Osteocyte lacunar density (n/mm^2)	831 ± 162
Mean osteon area (mm^2)	0.015 ± 0.004
Percentage porosity (%)	34.66 ± 19.1
Activation frequency (n/mm^2/year)	2.66 ± 1.50
Bone-formation rate (mm^3/mm^3/year)	0.04 ± 0.02

activation frequency and bone turnover were in agreement with previous studies on similar models [2, 8] and are reported in Table 2.

The percent of type 2 cracks was 66.2%, while percents for types 1 and 3–7 were 2.5%, 1.3%, 11.3%, 3.7%, 8.7%, and 6.3%, respectively. Type of microdamage and microdamage localization were not influenced by body mass or by sex (data not shown) according to the first GLM. No correlation was found between cortical microstructure and microcrack density and length.

The second GLM showed that bone mass is a good predictor for microcrack density, bone turnover is influenced only by age, whereas the cortical microstructural organization is not influenced by age, mass, or sex (Table 3). In our experimental settings sex did not influence any of the investigated variables. Figure 1 describes the relations between microcrack density and bone mass, between activation frequency and normalized age, and between bone-formation rate and normalized age through exponential equations.

Discussion

Damage accumulation is a normal response of composite materials to mechanical loading, and structure size is a recognized critical factor. In this study we investigated the effect of bone size on bone microdamage accumulation. We collected samples from pet dogs of a wide range of sizes in the second half of their expected life. We assumed their bones had been subjected daily to the low physiological cyclic loading consistent with pet lifestyle. Bones from animals that died at different ages were clearly subjected to a different number of cycles. However, we assumed that, under these loading conditions, the bones were in a phase of benign microdamage accumulation. In this phase we took a picture of the "characteristic damage state" of each bone in a balanced condition between the crack growth process and the repair process by bone turnover.

Table 3 General linear multivariate model

$R^2 = 0.63$	Dependent variables	F	P
Correct model	Microcrack density	**5.197**	**0.023**
	Microcrack mean length	0.650	0.602
	Percentage porosity	1.09	0.255
	Activation frequency	**6.268**	**0.014**
	Bone formation rate	**7.786**	**0.007**
	Mean osteon area	1.894	0.201
Normalized age	Microcrack density	0.013	0.910
	Microcrack mean length	0.640	0.444
	Percentage porosity	0.198	0.667
	Activation frequency	**9.991**	**0.012**
	Bone formation rate	**5.254**	**0.048**
	Mean osteon area	3.909	0.079
Bone mass	Microcrack density	**8.653**	**0.016**
	Microcrack mean length	0.812	0.391
	Percentage porosity	3.727	0.086
	Activation frequency	0.061	0.810
	Bone formation rate	3.188	0.108
	Mean osteon area	5.062	0.051
Sex	Microcrack density	0.013	0.910
	Microcrack mean length	0.639	0.444
	Percentage porosity	0.004	0.953
	Activation frequency	0.420	0.533
	Bone formation rate	0.278	0.611
	Mean osteon area	0.021	0.888

Model for histomorphometric parameters (dependent variables), normalized age and bone mass (covariates), and sex (fixed factor). Values statistically significant are highlighted in *bold*

Our results are reliable if compared to previous works performed on animals of the same size [17]. Male and female dogs of different size have the same cortical bone microstructural organization. Their tissue is equally damaged, and the characteristics of the damaged matrix are similar. The microcrack length in particular was found to be quite constant. The crack length is considered to reflect the magnitude of the cyclic loads applied [21]. Interspecies analyses have already demonstrated that microcrack length does not change with age [6, 22–26]. Our data confirm that the cyclic loading environment affecting a bone does not vary with biological age, as Frank et al. [2] already proposed, and that it does not vary with size within a single species.

Surprisingly, we found that age does not influence microdamage status. Previous studies showed that the sampling technique may highlight the mass or the age effect. Muir and Ruaux-Mason [8], for example, did not find any significant associations among age, body weight, and microcrack density and length in medium and large-breed dogs, while Frank et al. [2] found significant
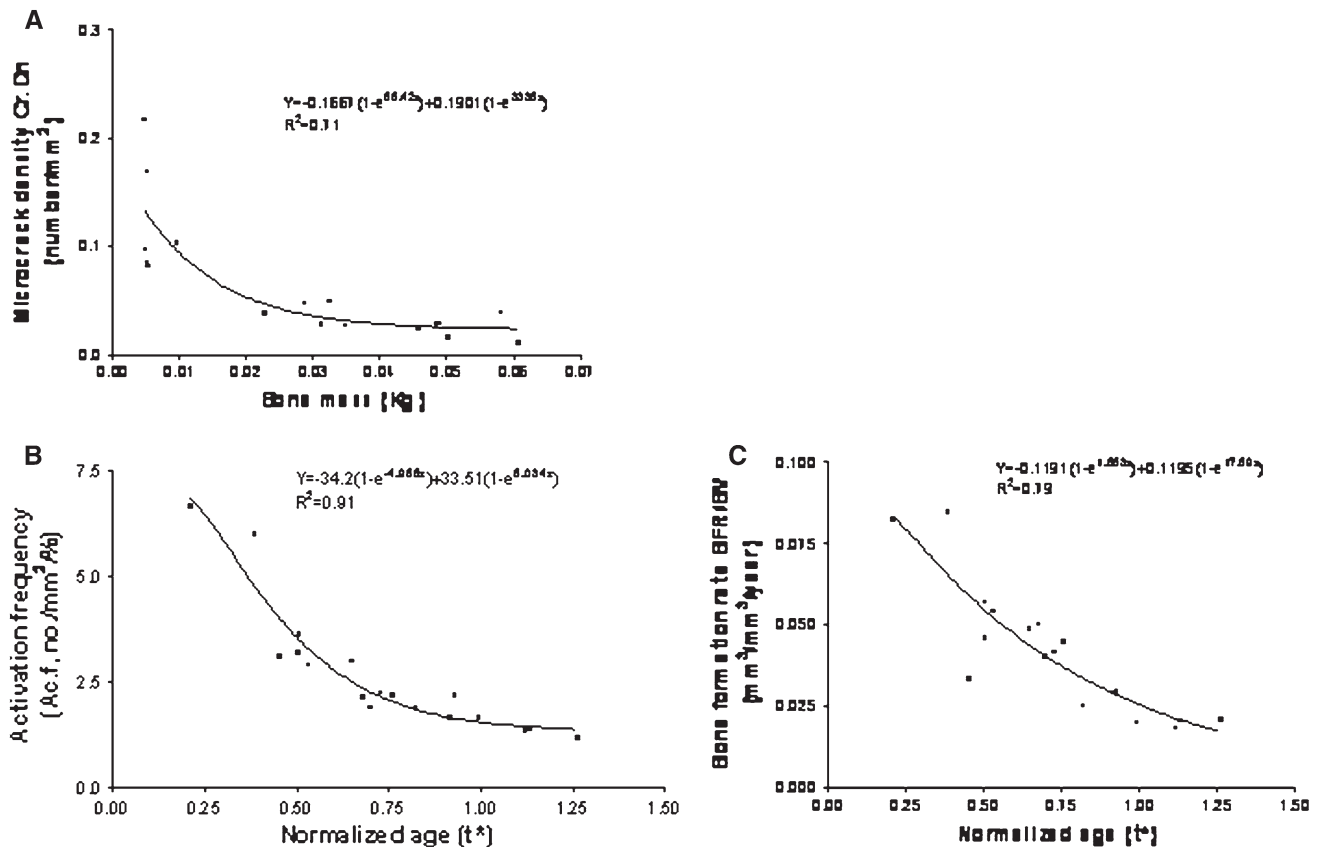
Fig. 1 The exponential equation describes the trend of microcrack density with respect to bone mass (**a**), the trend of activation frequency with respect to normalized age ($t*$) (**b**), and the trend of bone-formation rate (BFR/BV) with respect to normalized age ($t*$). Equations and R^2 are indicated

relationships between microdamage and age. In the population we examined, microdamage status worsened with age, but the correlation was not significant. Furthermore, the activity of the tissue, namely, the bone-formation rate and the acquisition frequency, decreased with age, both chronological and adjusted for life expectancy.

The bone turnover was similar in individuals of remarkably different mass, suggesting that the metabolic cost to maintain the bone healthy is size-invariant. Larger animals showed less microdamage accumulation, contradicting what we first expected and indirectly confirming that larger and small animals have the same risk of fatigue failure. We could expect a different tissue microscopic organization since some authors debated on the effect of osteon size on the control of crack propagation in cortical bone [27–29]. Some suggested that smaller and/or more osteons may better prevent catastrophic failure and slow the cracks, whereas others argued that osteon size does not influence work to failure [30, 31]. The general view is that cortical bone tends to fracture where there are fewer and smaller osteons and is tougher where osteon packing and size are greater. In the investigated population though, we found that the osteon size, the porosity, and the ostecyte lacunar density do not significantly change according to bone mass. The main finding of the current study is that the microdamage status decreases as the individual's mass increases; nevertheless, the investigated histomorphometric variables were not able to explain this result. We therefore hypothesize that some bone material properties, not under investigation in this work, change according to animal mass. In the appendix (supplementary material), we propose a theoretical explanation of how the bone tissue could dampen an increase in microdamage accumulation with an increase of the size of the bone structure.

When considering fatigue, it must be briefly recalled that body size has a profound impact on many aspects of animal physiology, including locomotion. On a mass-specific basis, small animals use stiffer legs [32] and more metabolic energy [33] than large animals to run a fixed distance. At their lowest galloping speed, small mammals sweep through larger hindlimb excursion angles [34] and use greater stride frequencies [35, 36]. Straightforward observation of walking or running dogs reveals that a small dog takes many more strides than a large dog to cover the same distance. The same fatigue life is perhaps optimized, requiring also proportionality to lifetime expectancy and

mean loading frequency (see Appendix as supplementary material). Since under physiological loading, bone remodeling is a mass-invariant process bent on removing microdamage at a constant rate, the behavior of large animals somehow offsets the disadvantages of size on bone fatigue properties. As the size increases, more time is required to perform a certain number of cycles and, thus, to accumulate a certain amount of microdamage.

This study has several limitations. It is founded on a small number of samples whose loading history can be only conjectured. In addition, conventional methods of measuring cracks on random transverse sections convey limited information, especially about crack shape [6]. Here, we assume that microcracks have an elliptical shape and a fixed aspect ratio (theoretical longitudinal: transverse = 5:1) [6, 37, 38]. Three-dimensional analysis may reveal different information on the strategy adopted by the bone tissue in order to cope with the size effect on its fatigue properties. Lastly, we assumed that exactly the same bone segment could be stained and analyzed and that the matrix material properties were characteristic of each bone mass, while it was also demonstrated that fracture toughness depends on bone location [39].

In conclusion, we found bones from animals belonging to the same species, but of remarkably different size, to have similar cortical microstructural organization not associated with a mass-related increase in bone-formation rate. In larger bones there is a higher probability of finding a weak region where a crack can arise and grow. As we demonstrated, this is not the case within the same species as we found an exponential decrease of the microdamage density as bone mass increase. In the appendix (supplementary material) [40, 41] we theoretically propose a mass-related change in the material fracture toughness. We suggest tuning at the molecular and supramolecular levels during tissue morphogenesis targeted to reach an optimal unique dimensionless curve for fatigue life. While supporting Taylor's interspecific hypothesis, we also extend his conclusions in the intraspecific field by means of a model based on the "quantized" Paris law.

References

1. Schaffler MB, Choi K, Milgrom C (1995) Aging and matrix microdamage accumulation in human compact bone. Bone 17:521–525
2. Frank JD, Ryan M, Kalscheur VL, Ruaux-Mason CP, Hozak RR, Muir P (2002) Aging and accumulation of microdamage in canine bone. Bone 30:201–206
3. Muir P, Johnson KA, Ruaux-Mason CP (1999) In vivo matrix microdamage in a naturally occurring canine fatigue fracture. Bone 25:571–576
4. Martin RB, Stover SM, Gibson VA, Gibeling JC, Griffin LV (1996) In vitro fatigue behavior of the equine third metacarpus: remodeling and microcrack damage analysis. J Orthop Res 14:794–801
5. Nunamaker DM, Butterweck DM, Provost MT (1990) Fatigue fractures in thoroughbred racehorses: relationships with age, peak bone strain, and training. J Orthop Res 8:604–611
6. Taylor D, Lee TC (1998) Measuring the shape and size of microcracks in bone. J Biomech 31:1177–1180
7. Wayne RK, Ostrander EA (1999) Origin, genetic diversity, and genome structure of the domestic dog. Bioessays 21:247–257
8. Muir P, Ruaux-Mason CP (2000) Microcrack density and length in the proximal and distal metaphyses of the humerus and radius in dogs. Am J Vet Res 61:6–8
9. Forwood MR, Parker AW (1989) Microdamage in response to repetitive torsional loading in the rat tibia. Calcif Tissue Int 45:47–53
10. Brianza SZ, D'Amelio P, Pugno N, Delise M, Bignardi C, Isaia G (2007) Allometric scaling and biomechanical behavior of the bone tissue: an experimental intraspecific investigation. Bone 40:1635–1642
11. Brianza SZ, Delise M, Maddalena Ferraris M, D'Amelio P, Botti P (2006) Cross-sectional geometrical properties of distal radius and ulna in large, medium and toy breed dogs. J Biomech 39:302–311
12. Li Y, Deeb B, Pendergrass W, Wolf N (1996) Cellular proliferative capacity and life span in small and large dogs. J Gerontol A Biol Sci Med Sci 51:B403–B408
13. Patronek GJ, Waters DJ, Glickman LT (1997) Comparative longevity of pet dogs and humans: implications for gerontology research. J Gerontol A Biol Sci Med Sci 52:B171–B178
14. Greer KA, Canterberry SC, Murphy KE (2007) Statistical analysis regarding the effects of height and weight on life span of the domestic dog. Res Vet Sci 82:208–214
15. Parfitt AM, Drezner MK, Glorieux FH, Kanis JA, Malluche H, Meunier PJ, Ott SM, Recker RR (1987) Bone histomorphometry: standardization of nomenclature, symbols, and units. Report of the ASBMR Histomorphometry Nomenclature Committee. J Bone Miner Res 2:595–610
16. Burr DB, Stafford T (1990) Validity of the bulk-staining technique to separate artifactual from in vivo bone microdamage. Clin Orthop Relat Res 260:305–308
17. Norman TL, Wang Z (1997) Microdamage of human cortical bone: incidence and morphology in long bones. Bone 20:375–379
18. Vashishth D, Verborgt O, Divine G, Schaffler MB, Fyhrie DP (2000) Decline in osteocyte lacunar density in human cortical bone is associated with accumulation of microcracks with age. Bone 26:375–380
19. Stout SD, Paine RR (1994) Bone remodeling rates: a test of an algorithm for estimating missing osteons. Am J Phys Anthropol 93:123–129
20. Hattner R, Frost HM (1963) Mean skeletal age: its meaning and a method of calculation. Henry Ford Hosp Med Bull 11:201–216
21. Taylor D, Lee TC (2003) Microdamage and mechanical behaviour: predicting failure and remodelling in compact bone. J Anat 203:203–211
22. Rubin CT (1984) Skeletal strain and the functional significance of bone architecture. Calcif Tissue Int 36(Suppl 1):S11–S18
23. Rubin CT, Lanyon LE (1982) Limb mechanics as a function of speed and gait: a study of functional strains in the radius and tibia of horse and dog. J Exp Biol 101:187–211
24. Fazzalari NL, Forwood MR, Manthey BA, Smith K, Kolesik P (1998) Three-dimensional confocal images of microdamage in cancellous bone. Bone 23:373–378

25. Burr DB, Milgrom C, Fyhrie D, Forwood M, Nyska M, Finestone A, Hoshaw S, Saiag E, Simkin A (1996) In vivo measurement of human tibial strains during vigorous activity. Bone 18:405–410
26. Schaffler MB, Radin EL, Burr DB (1989) Mechanical and morphological effects of strain rate on fatigue of compact bone. Bone 10:207–214
27. Moyle DD, Welborn JW III, Cooke FW (1978) Work to fracture of canine femoral bone. J Biomech 11:435–440
28. Barth RW, Williams JL, Kaplan FS (1992) Osteon morphometry in females with femoral neck fractures. Clin Orthop Relat Res 283:178–186
29. Yeni YN, Brown CU, Wang Z, Norman TL (1997) The influence of bone morphology on fracture toughness of the human femur and tibia. Bone 21:453–459
30. Moyle DD, Bowden RW (1984) Fracture of human femoral bone. J Biomech 17:203–213
31. Corondan G, Haworth WL (1986) A fractographic study of human long bone. J Biomech 19:207–218
32. Farley CT, Glasheen J, McMahon TA (1993) Running springs: speed and animal size. J Exp Biol 185:71–86
33. Taylor CR, Schmidt-Nielsen K, Raab JL (1970) Scaling of energetic cost of running to body size in mammals. Am J Physiol 219:1104–1107
34. McMahon TA (1975) Using body size to understand the structural design of animals: quadrupedal locomotion. J Appl Physiol 39:619–627
35. Heglund NC, Taylor CR, McMahon TA (1974) Scaling stride frequency and gait to animal size: mice to horses. Science 186:1112–1113
36. Gasc JP (2001) Comparative aspects of gait, scaling and mechanics in mammals. Comp Biochem Physiol A Mol Integr Physiol 131:121–133
37. Burr DB, Martin RB (1993) Calculating the probability that microcracks initiate resorption spaces. J Biomech 26:613–616
38. O'Brien FJ, Taylor D, Dickson GR, Lee TC (2000) Visualisation of three-dimensional microcracks in compact bone. J Anat 197(3):413–420
39. Brown CU, Yeni YN, Norman TL (2000) Fracture toughness is dependent on bone location—a study of the femoral neck, femoral shaft, and the tibial shaft. J Biomed Mater Res 49:380–389
40. Pugno N (2006) New quantized failure criteria: application to nanotubes and nanowires. Int J Fract 141:311–328
41. Pugno MC, Cornetti P, Carpinteri A (2006) A unified law for fatigue crack growth. J Mech Phys Solids 54:1333–1349